

The effect of structural variability and local site conditions on building fragility functions

Aida Azari Sisi^{*1}, Murat A. Erberik^{2a} and Ayşegül Askan^{2a}

¹Federal Institute for Geoscience and Natural Resources (BGR), Hannover, Germany

²Department of Civil Engineering, Middle East Technical University, Ankara, Turkey

(Received November 20, 2017, Revised February 17, 2018, Accepted February 19, 2018)

Abstract. In this study, the effect of local site conditions (site class and site amplifications) and structural variability are investigated on fragility functions of typical building structures. The study area is chosen as Eastern Turkey. The fragility functions are developed using site-specific uniform hazard spectrum (UHS). The site-specific UHS is obtained based on simulated ground motions. The implementation of ground motion simulation into seismic hazard assessment has the advantage of investigating detailed local site effects. The typical residential buildings in Erzincan are represented by equivalent single degree of freedom systems (ESDOFs). Predictive equations are accomplished for structural seismic demands of ESDOFs to derive fragility functions in a straightforward manner. To study the sensitivity of fragility curves to site class, two sites on soft and stiff soil are taken into account. Two alternative site amplification functions known as generic and theoretical site amplifications are examined for these two sites. The reinforced concrete frames located on soft soil display larger fragilities than those on stiff soil. Theoretical site amplification mostly leads to larger fragilities than generic site amplification more evidently for reinforced concrete buildings. Additionally, structural variability of ESDOFs is generally observed to increase the fragility especially for rigid structural models.

Keywords: fragility functions; ground motion simulation; site effects

1. Introduction

Fragility functions represent the exceedance probability of any limit state as a function of ground motion intensity parameter (GMIP) (Porter 2003, Wen *et al.* 2004). They have been used extensively for the purposes of risk assessment in pre-earthquake periods and for the purposes of damage and loss assessment in post-earthquake periods. Numerous building fragility functions have been developed in different earthquake-prone countries by considering local structural characteristics, including Turkey (Erberik 2008a, Erberik 2008b, Ay and Erberik 2008).

Sensitivity of fragility curves to different parameters is a very significant issue. Erberik (2008a) addressed the considerable effect of degradation characteristics and limit state definitions on fragility functions of Turkish RC structures. Celik and Ellingwood (2010) studied the impact of structural uncertainties on demand predictions and fragility functions. The same authors derived two sets of structural models from mean parameters and parameter uncertainties. They compared the fragility curves related to two separate models. The sensitivity of bridge fragility assessment to uncertain bridge parameters was investigated by Padgett and DesRoches (2007). Mosleh *et al.* (2016) studied the fragility curves of reinforced concrete bridges for different earthquake sources mechanisms (strike-slip

and reverse). Jeong *et al.* (2015) discussed the impact of masonry infills on fragility functions of RC frames. The fragility functions of reinforced concrete beam-column connections were compared before and after rehabilitation by Marthong *et al.* (2016). Crowley *et al.* (2005) performed an intensive sensitivity analyses of seismic loss of typical structures in Marmara region, Turkey. The uncertainties which were used in Crowley *et al.* (2005) are related to site classification definitions, building classifications, demand spectrum and etc. Among the uncertainties which affect structural vulnerability, some of them are more important than the others. This issue was investigated thoroughly by Rohmer *et al.* (2014) for structural loss assessment in France. Nagashree *et al.* (2016) considered different material strength and damage state thresholds in fragility functions of reinforced concrete buildings.

Fragility curves can be derived by using real or simulated ground motions. For the estimation of GMIPs, using synthetic ground motions rather than ground motion prediction equations enables the inclusion of complex source effects (such as forward directivity), path effects (such as duration) and detailed local site effects in seismic hazard and risk assessment studies. Besides, ground motion prediction equations (GMPEs) are sometimes not capable of producing satisfactory results in regions with sparse data (e.g., Akansel *et al.* 2014, Raschke 2014). In particular, the effective role of site response in seismic hazard assessment was highlighted in previous studies (e.g., Cramer 2006, Hashash and Moon 2011). Most GMPEs consider rough site categories such as rock and soil (e.g., Ambraseys *et al.* 2005, Akkar and Bommer 2010). As a result, use of

*Corresponding author, Ph.D.

E-mail: aida.azarisisi@bgr.de

^aProfessor

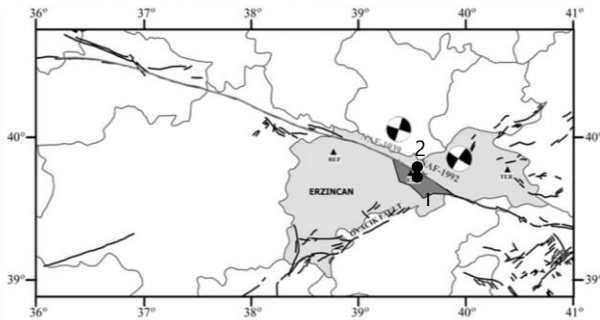


Fig. 1 Regional map showing the epicenters, rupture zones and the mechanisms of the 1939 and 1992 earthquakes (epicenters are indicated with stars) and strong ground motion stations that recorded 1992 Erzincan earthquake (indicated with triangles). The sites which are used in this paper are indicated with solid circles

simulated ground motions instead of GMPEs in probabilistic seismic hazard analyses becomes a valid option. Ground motion simulation was applied to estimate seismic loss by several researchers (e.g., Ellingwood *et al.* 2007, Ansal *et al.* 2009, Ugurhan *et al.* 2011).

The main goal of this study is to investigate the sensitivity of building fragility functions as well as mean damage ratios to local site conditions in Erzincan region by using simulated ground motions. The effect of site conditions includes the combined effects of site class and alternative site amplification functions. The most common building types in Erzincan are represented by ESDOF systems. The demand prediction equations of ESDOFs are derived using the selected ground motions with respect to site-specific UHS which is based on ground motion simulation. The fragility functions are determined using seismic demand prediction equations and reliability formulation. Besides, the mean and variance of structural parameters of ESDOF models are examined separately to assess the influence of structural variability on fragility functions.

2. Site-specific seismic hazard assessment based on simulated ground motions

The Erzincan region in Eastern Turkey is selected as the case study area in this paper. Erzincan city is located in a tectonically very complex regime (Fig. 1). Two sites are selected in this region. Site 1 is Erzincan city center, which is located on soft soil. Site 2 is inside Erzincan city near Cumhuriyet district, which is located on stiff soil.

The coordinates and other properties of the seismic zones are derived from Deniz (2006). There are nine seismic zones consisting of five fault zones and four areal seismic zones (i.e., background zones) in the region of interest. Table 1 and Fig. 2 show the seismic properties and locations of these seismic zones, respectively.

As the first step, the events are distributed within time spans using Monte Carlo simulation method and magnitude of each event is calculated through Gutenberg-Richter recurrence model. The epicenters of events are distributed

Table 1 Seismic parameters of the seismic zones used in this study (Adopted from Deniz 2006)

No	Name	M_{\max}	M_{\min}	Average Depth (km)	λ	β
1	North Anatolian Fault Zone-Segment D	8.0	4.5	25.0	1.07	1.35
2	East Anatolian Fault Zone	7.5	4.5	24.3	2.16	2.14
3	North East Anatolian Fault Zone	7.8	4.5	22.2	1.14	2.16
4	Central Anatolian Fault Zone	7.1	4.5	20.1	0.56	2.74
5	Yazyurdu-Goksun Fault Zone	7.0	4.5	20.3	1.01	3.43
6	Background Inner 3	5.4	4.5	6.7	0.08	2.20
7	Background Inner 4	5.4	4.5	22.2	0.64	2.63
8	Background North	5.8	4.5	18.5	0.74	3.30
9	Background Inner 5	5.6	4.5	36.6	1.99	2.40

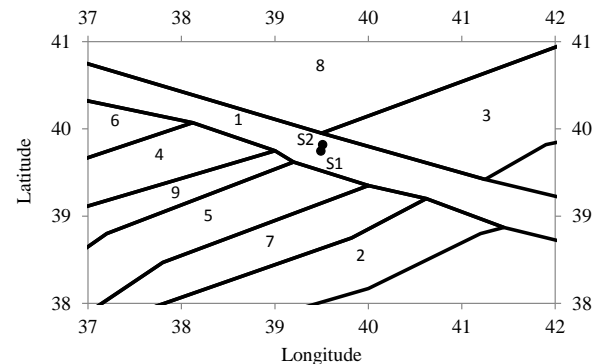


Fig. 2 Locations of seismic zones which are used in this study. The sites under study are shown with solid circles with their numbers

randomly inside each seismic zone. Two random numbers for latitude and longitude are generated inside the borders of each source. Next, ground motion time histories due to seismic waves propagating from epicenters to the site of interest, are simulated. The ground motions of events that occur on the faults are modeled using stochastic finite-fault model based on dynamic corner frequency proposed by Motazedian and Atkinson (2005). For areal sources, stochastic point source method is used following the approach outlined in Boore (2003).

Values of geometric spreading, quality factor, high frequency decay factor and ground motion duration are adopted from Askan *et al.* (2013). The authors of that study validated the aforementioned parameters by simulating records of the 13 March Erzincan 1992 ($M_w=6.6$) earthquake. Rupture dimensions are estimated from the empirical relationships defined by Wells and Coppersmith (1994). Stress drop is estimated from the empirical relations in Mohammadioun and Serva (2001) that relate its value to rupture dimensions. Finally, EXSIM and SMSIM computer programs are used to model extended faults and point sources, respectively.

Two alternative approaches are applied in this paper to characterize site response. The first one is generic site amplification proposed by Boore and Joyner (1997), which

is based on local V_{s30}^1 at sites of interest. The second approach is the theoretical site amplification, which is based on transfer functions computed for layered earth models. One-dimensional (1D) standard site response analysis is employed for soil profiles to develop transfer functions using SHAKE software (Schnabel *et al.* 1972). A bedrock ground motion with $PGA=0.002$ g is applied as input to calculate the theoretical site amplification.

As the final step, response spectrum of the simulated ground motions is calculated for specified periods. Then ground motion amplitudes related to each period are sorted from largest to smallest, the first value has annual exceedance rate of $1/n$, the second value has annual exceedance rate of $2/n$ and so on where n is catalog period in terms of years. The ground motion amplitudes related to the same hazard level for the entire period range yields site-specific UHS. The ground motions are selected from the simulated ground motion catalog which is used for seismic hazard calculations. The selected ground motions have minimum deviation from the proposed UHS. Four hazard levels of 2%, 10%, 20% and 50% exceedance probabilities in 50 years are taken into account. Twenty ground motions records are selected for each hazard level. The related procedures to obtain regional seismic hazard functions are described in detail by Azari Sisi *et al.* (2017).

3. Dynamic analysis of ESDOF models

In this study, six ESDOF models to represent the corresponding typical building classes are taken into account, which consist of low- and mid-rise reinforced concrete (RC) frames as well as unreinforced masonry (URM) buildings with one, two and three stories. These ESDOF models represent the most common building structures in the study region.

3.1 Methodology

The ESDOF classes used in this study are determined via detailed field observations in Erzincan within the context of a national research project (Askan *et al.* 2015). The abbreviations of the building classes are RF1A, RF2B, RF2C, MU1A, MU2B and MU3C. The letters “RF” and “MU” in these codes stand for RC frame and URM structures, respectively. Numbers “1” and “2” in abbreviations of the RF classes denote low-rise and mid-rise structures, respectively. For MU classes, numbers “1”, “2” and “3” directly stand for the number of stories. Finally, the letters “A”, “B” and “C” respectively represent high, moderate and low levels of conformity of the considered building class to the modern principles of seismic design codes. The six ESDOF models in this study cover a wide range of existing building structures in the study region with different construction types, number of stories and structural response characteristics. Peak-oriented hysteretic model of Ibarra *et al.* (2005) is used to simulate the

Table 2 The characteristics of the ESDOF models (Askan *et al.* 2015)

Sub-class	$T(s)$		η		μ		$\alpha_s(\%)$	$\alpha_c(\%)$	λ	γ
	MN	STD	MN	STD	MN	STD				
RF1A	0.38	0.18	0.40	0.08	9.0	3.1	4	-20	0.2	800
RF2B	0.70	0.27	0.26	0.09	6.1	1.7	4	-25	0.2	400
RF2C	0.70	0.27	0.17	0.06	5.1	1.4	4	-30	0.2	200
MU1A	0.06	0.02	0.86	0.17	3.5	0.7	0	-20	0.2	600
MU2B	0.11	0.03	0.43	0.11	2.6	0.7	0	-25	0.2	300
MU3C	0.17	0.05	0.14	0.04	2.1	0.6	0	-30	0.2	150

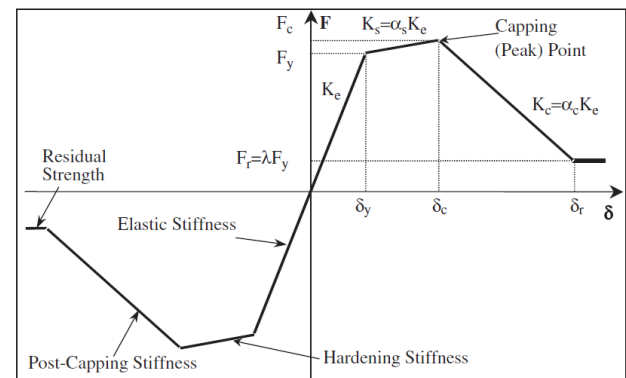


Fig. 3 The backbone curve of peak-oriented hysteretic model (Ibarra *et al.* 2005)

hysteresis relationship of the ESDOF models. The backbone curve of this model is shown in Fig. 3 with all the model parameters. Table 2 gives the values of the major model parameters, which has been taken from Askan *et al.* (2015).

In Table 2, there exist three random variables in order to simulate the structural variability. These random variables with mean (MN) and standard deviation (STD) values include the effective period (T), yield strength ratio (η) and ductility ratio (μ). In addition, the constant-valued model parameters are post-yield stiffness ratio (α_s), post-capping stiffness ratio (α_c), strength reduction factor (λ) and hysteretic energy dissipation capacity (γ).

The ESDOF systems are modeled through OPENSEES platform. Nonlinear time history analysis is performed using the selected simulated ground motions. The ground motions corresponding to 2% exceedance probability in 50 years related to Site 1, generally cause unphysically large structural demands because of their vicinity to NAFZ and soft soil conditions. Hence this hazard level is disregarded for Site 1.

Predictive equations are developed for structural seismic demand as a function of earthquake intensity. Regression analysis is preferred over lognormal distribution fitting in this study because the selected ground motions for different hazard levels lead to cloud demand scatters (Celik and Ellingwood 2010). Besides, using demand predictive models enables more practical calculations for fragility curves through reliability formulation. The predictive model has the functional form of Eq. (1) referring to previous studies (e.g., Krawinkler *et al.* 2003, Ramamoorthy *et al.* 2006, Ellingwood *et al.* 2007, Ramamoorthy *et al.* 2008, Bai *et al.* 2011).

¹Average shear-wave velocity for the top 30 m of the subsurface profile

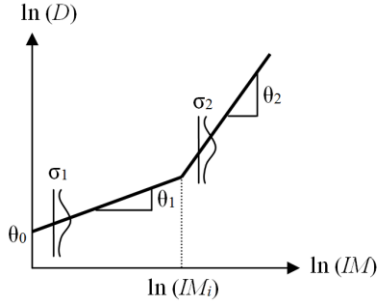


Fig. 4 Schematic illustration of bilinear demand model (Adapted from Bai *et al.* 2011)

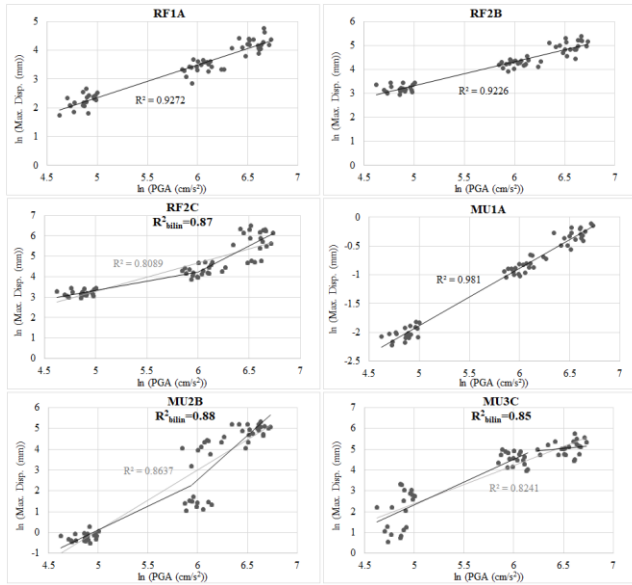


Fig. 5 Variation of maximum displacement demand with respect to PGA and the predictive regression models for Site 1 using generic site amplification

$$\ln(D) = \theta_0 + \theta_1 \ln(IM) + \sigma \varepsilon \quad (1)$$

D and IM stand for structural demand and ground motion intensity measure, respectively. In this study, maximum displacement is considered as the main structural demand parameter and peak ground acceleration (PGA) is selected as ground motion intensity parameter. The ε term in Eq. (1) is a random variable with zero mean and unit standard deviation. Parameter σ is standard deviation of model errors.

In some cases, $\ln(D)$ - $\ln(IM)$ scatters do not follow a linear trend. Hence Eq. (1) is not adequate for these cases since it underestimates or overestimates the observed data. Some researchers proposed to use bilinear trend in this case similar to Eq. (2) (e.g., Ramamoorthy *et al.* 2006, Ramamoorthy *et al.* 2008, Bai *et al.* 2011). Fig. 4 illustrates schematic form of bilinear model.

$$\begin{aligned} \ln(D) &= \theta_0 + \theta_1 \ln(IM) + \sigma_1 \varepsilon_1 & IM \leq IM_1 \\ \ln(D) &= [\theta_0 + \theta_1 \ln(IM_1)] + \theta_2 [\ln(IM) - \ln(IM_1)] + \sigma_2 \varepsilon_2 & IM > IM_1 \end{aligned} \quad (2)$$

Standard least square regression methodology is applied to estimate parameters θ_0 , θ_1 , θ_2 , σ_1 and σ_2 in Eqs. (3) and (4).

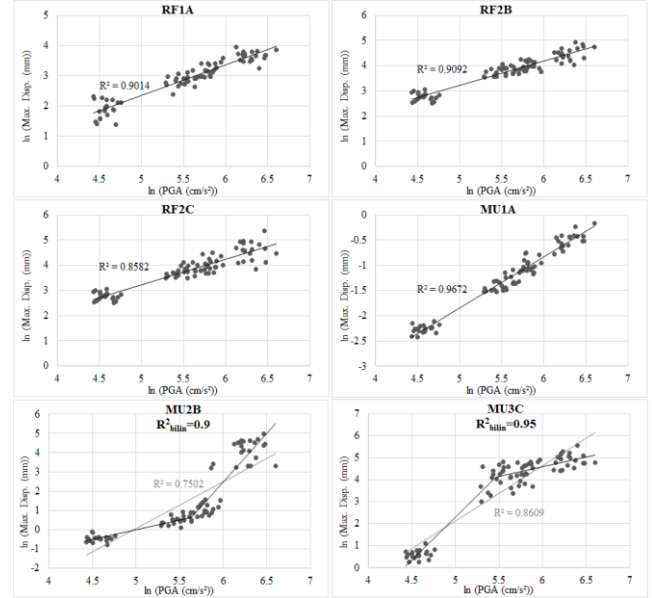


Fig. 6 Variation of maximum displacement demand with respect to PGA and the predictive regression models for Site 2 using generic site amplification

3.2 Demand predictive equations of ESDOFs without structural variability

Figs. 5 and 6 show the structural demand variations with respect to PGA as well as the predictive equations for two sites with different site amplification models. Mean values of T , η and μ in Table 2 are used in Figs. 5 and 6 thus the structural variability is disregarded. As it was mentioned previously, bilinear predictive models are preferred for some ESDOFs. For such cases, original linear model is also shown in grey to observe the difference.

It is observed from Figs. 5 and 6 that, in some of the cases (i.e., for RF2C, MU2B and MU3C classes) bilinear predictive models are required. The common characteristics of these ESDOF models is that they demonstrate severe deterioration characteristics (they have the smallest γ 's). R^2_{bilin} , which is the corresponding R^2 value for bilinear models, is improved especially for Site 2 after modifying the predictive linear models into bilinear form. It should be noted that, the intersection point of two lines regarding bilinear models is selected by trial and error procedures to give the largest R^2 .

The second slope is greater than the first one for RF2C and MU2B models. Therefore, as PGA increases, demand is increasing more rapidly for large ground motion amplitudes. The second slope is smaller than the first one for MU3C model. Regarding this model, as PGA increases, demand is increasing more slowly for high ground motion intensity values than low ones. In other words, rare events with return periods of 2475 or 475 years are more critical for MU2B and RF2C. However, frequent events with return periods of 225 or 75 years are more critical for MU3C, which is the most vulnerable building class among all.

3.3 Demand predictive equations of ESDOFs with structural variability

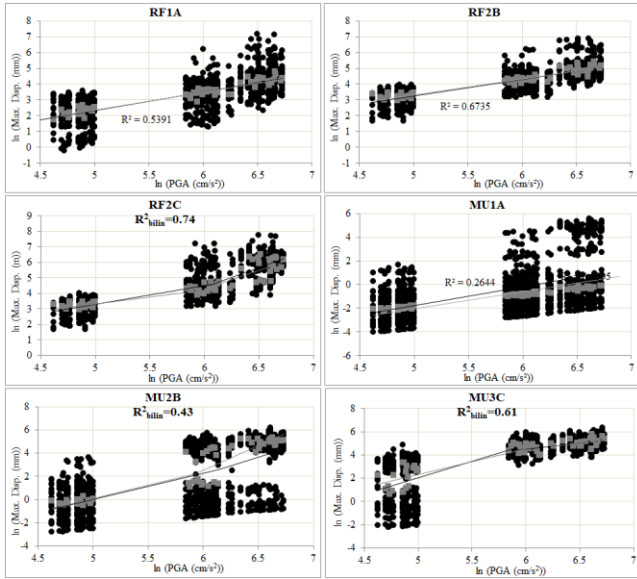


Fig. 7 Variation of maximum displacement demand with respect to PGA and the predictive regression models for Site 1 using generic site amplification

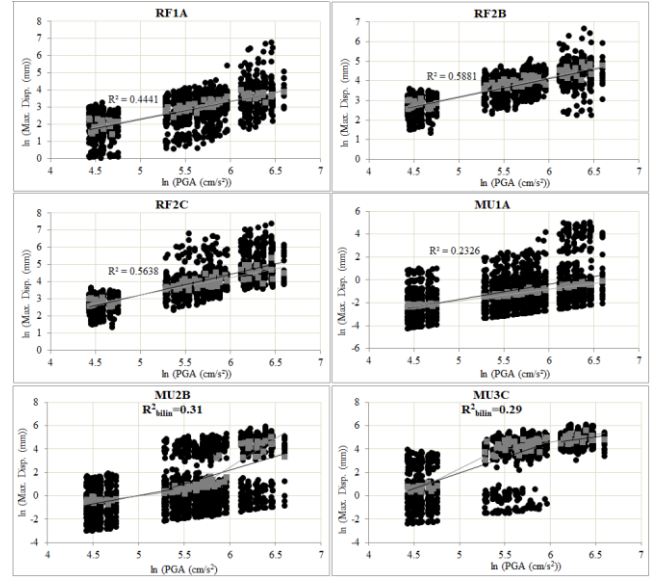


Fig. 8 Variation of maximum displacement demand with respect to PGA and the predictive regression models for Site 2 using generic site amplification

The probabilistic distributions of structural parameters (T , η and μ) are taken into account for modeling ESDOFs using Latin Hypercube Sampling (LHS) method. Those three parameters are regarded as random variables with mean and standard deviation properties since they affect the fragility functions more than other parameters. LHS methodology is developed by McKay *et al.* (1979) and is preferred by several authors (Ayyub and Lai 1989, Erberik, 2008a, Askan *et al.* 2015). This approach is proved by McKay *et al.* (1979) to capture the complete probabilistic distribution properly with a limited number of samples as compared to Monte Carlo Method.

The time history analyses are repeated for 20 simulations obtained from LHS regarding each ESDOF class. The structural demand variations of ESDOFs with respect to PGA are shown in Figs. 7 and 8 as well as demand predictive models. The scatters and predictive equations related to the building cases without structural variability are also exhibited in grey.

Figs. 7 and 8 indicate that, median predictive demands remain almost unchanged after considering structural variability for RF1A and RF2B. However, there is a significant increase in median demands after considering structural variability regarding some ESDOF systems like MU1A. Figs. 7 and 8 show median regression models, however, dispersion of regression models is not present in the figures. Dispersion of predictive model is defined as logarithmic uncertainty ($\beta_{D/IM}$) related to predicted demand given intensity measure, which is computed through Eq. (3) (Wen *et al.* 2004).

$$\beta_{D/IM} = \sqrt{\ln\left(1 + \frac{\sum [\ln(D_{obs}) - \ln(\hat{D})]^2}{n - 2}\right)} \quad (3)$$

where D_{obs} is observed displacement demand, D is median demand which is estimated from regression analyses and n is sample size. Structural variability increases dispersion

values considerably. This observation is expected because number of data (n in Equation 3) is increased to a great extent.

4. Parametric study on fragility functions

Fragility functions are derived using the well-known reliability formulation as Eq. (4) (Ang and Tang 1975)

$$P(LS_i | GMIP) = 1 - \Phi\left(\frac{\ln(\hat{C}) - \ln(\hat{D})}{\sqrt{\beta_C^2 + \beta_{D/IM}^2 + \beta_M^2}}\right) \quad (4)$$

where $P(LS_i | GMIP)$ is exceedance probability of i^{th} limit state given the ground motion intensity parameter. Φ is cumulative standard normal distribution. D and $\beta_{D/IM}$ are median demand and demand uncertainty in logarithmic scale, respectively. These two parameters are estimated from regression analyses. Parameters C and β_C are median capacity and variability in capacity dispersion in terms of displacement for i^{th} limit state, respectively. It is a quite challenging task to obtain C values. The values shown in Table 3 have been determined after a significant effort by considering previous research, field observations and numerical studies on the mentioned building classes as it is explained in detail by Askan *et al.* (2015).

Parameter β_C is assumed by considering the available literature. Wen *et al.* (2004) stated that the value $\beta_C=0.3$ is appropriate for limit states which are derived from pushover analysis. This is also the average of dispersion values which are used by Erberik (2008a). Besides, Ramamoorthy *et al.* (2008) made use of $\beta_C=0.3$ in calculating fragility curves. Therefore capacity dispersion is assumed to be 0.3 in this study.

β_M is epistemic portion of uncertainty related to modeling. The most important source of epistemic uncertainty is idealization of buildings as ESDOFs. This

Table 3 Limit state median capacity in terms of displacement for ESDOFs (Askan *et al.* 2015)

	limit state	Mean S_d (cm)
RF1A	LS1 (low damage)	1.55
	LS2 (intermediate damage)	6.70
	LS3 (high damage)	12.40
RF2B	LS1 (low damage)	2.00
	LS2 (intermediate damage)	8.10
	LS3 (high damage)	15.20
RF2C	LS1 (low damage)	1.65
	LS2 (intermediate damage)	7.11
	LS3 (high damage)	14.30
MU1A	LS1 (low damage)	0.07
	LS2 (intermediate damage)	0.25
	LS3 (high damage)	1.54
MU2B	LS1 (low damage)	0.14
	LS2 (intermediate damage)	0.37
	LS3 (high damage)	1.67
MU3C	LS1 (low damage)	0.11
	LS2 (intermediate damage)	0.52
	LS3 (high damage)	1.88

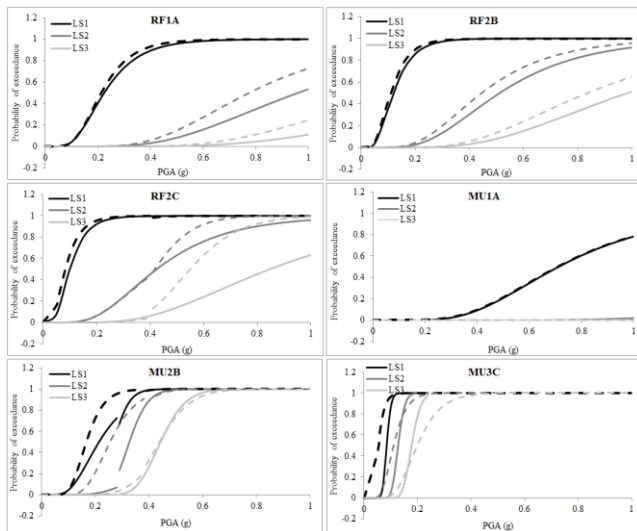


Fig. 9 Fragility curves related to Site 2 (solid line) and Site 1 (dashed line)

parameter is also assumed by examining the values in literature. Wen *et al.* (2004) compared fragilities of RC frames for $\beta_M=0.2, 0.3$ and 0.4 and observed no significant difference. They assumed later 0.3 for this parameter. Ellingwood *et al.* (2007) assumed $\beta_M=0.2$ for fragility calculations. In this study, modeling uncertainty is assumed to be 0.3 .

Fig. 9 displays fragility functions of Site 1 and Site 2 using generic site amplification for ESDOFs without structural variability. The main goal of this figure is to show the effect of site class on fragility curves.

The comparison of the fragility curve sets in Fig. 9 reveals that RF sub-class on soft soil (Site 1) are more fragile than the ones on stiff soil (Site 2). The difference in fragilities even becomes more significant for deficient sub-

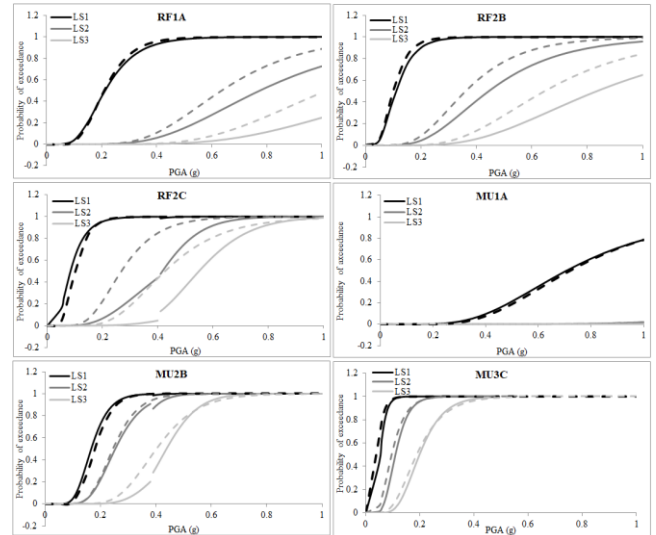


Fig. 10 Fragility curves related to Site 1 using generic (solid line) and theoretical (dashed line) site amplification function

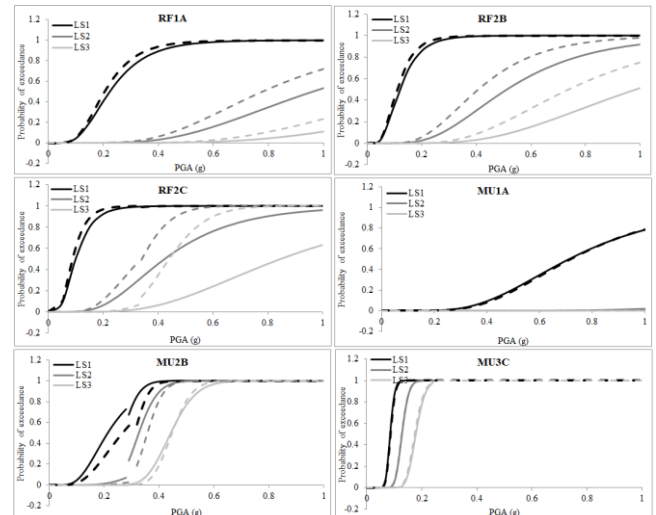


Fig. 11 Fragility curves related to Site 2 using generic (solid line) and theoretical (dashed line) site amplification function

class (i.e., RF2C). This trend is in accordance with the field observations after major earthquakes in which most of the deficient RC frame buildings in districts with soft soil condition have either experienced severe damage or collapse. For masonry buildings, the trend seems to be different due to the dynamic characteristics of these building sub-classes. Since masonry buildings are generally rigid structures, it may be expected that they are influenced when they reside on stiff soil conditions, especially if they have been constructed in a non-engineered manner.

Fragility functions of Site 1 and 2 are recomputed using theoretical site amplification. Fragility curves using theoretical site amplification are compared with the ones using generic one in Figs. 10 and 11.

Fig. 10 indicates that, theoretical site amplification increases fragilities for RC frames, considerably. This increase becomes more apparent for the second and third

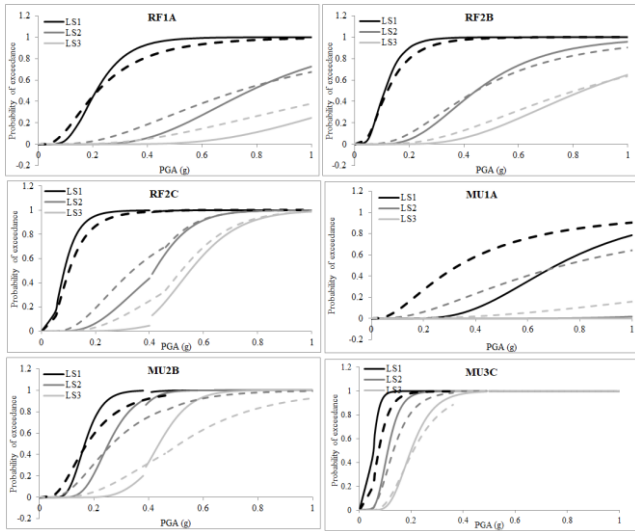


Fig. 12 Fragility curves related to Site 1 using generic site amplification without (solid line) and with (dashed line) structural variability

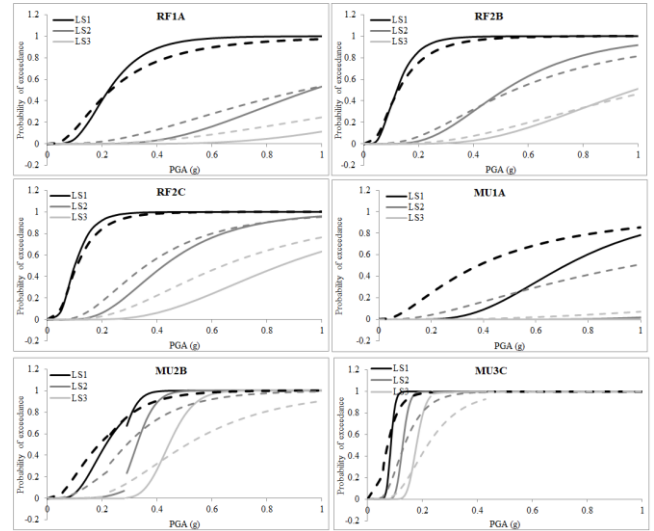


Fig. 14 Fragility curves related to Site 2 using generic site amplification without (solid line) and with (dashed line) structural variability

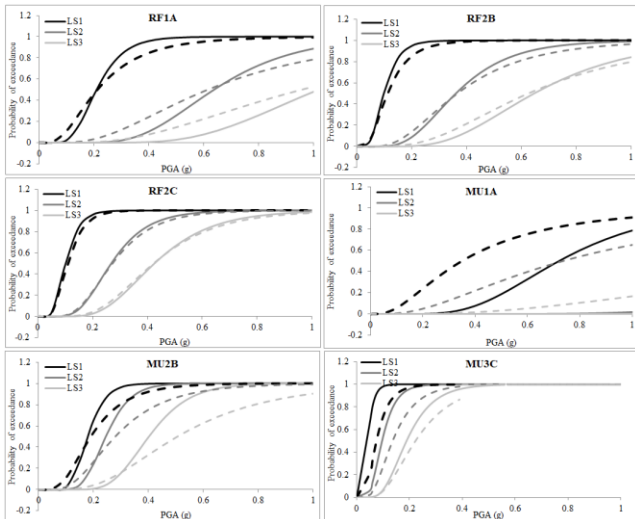


Fig. 13 Fragility curves related to Site 1 using theoretical site amplification without (solid line) and with (dashed line) structural variability

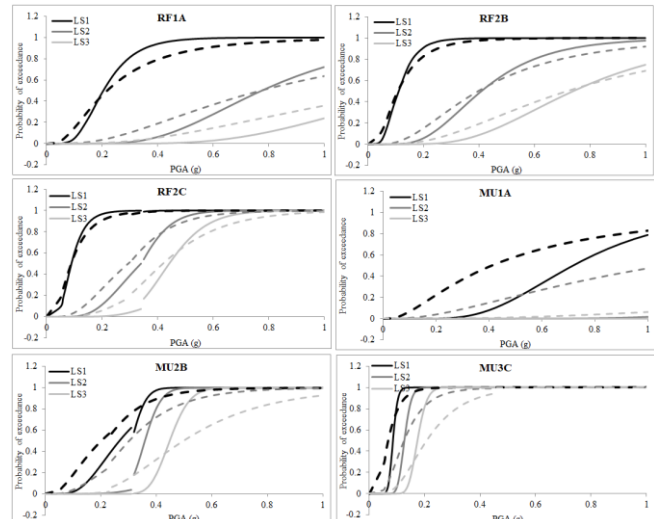


Fig. 15 Fragility curves related to Site 2 using theoretical site amplification without (solid line) and with (dashed line) structural variability

limit states of RF2C because of severe deterioration characteristics. The effect of theoretical site function on masonry models is not as considerable as RC frames even it decreases fragilities for some limit states. The main reason is that, theoretical site amplification has complex behavior and considerably larger peaks than generic site amplification for low frequencies (Azari Sisi *et al.* 2017)

The results of Fig. 11 related to Site 2 are to some extent similar to Fig. 10 of Site 1. Considerable and negligible difference between fragilities is observed for RC frames and masonry models, respectively. Theoretical site amplification increases fragilities of RF2C for Site 2 much more than Site 1. The difference between theoretical and generic site amplifications at low frequencies of Site 2 is more than that of Site 1. Besides, the structures with high deterioration are affected by detailed site response more than other structural models.

Next, structural variability of each ESDOF sub-class is taken into account using Latin hypercube sampling method. The obtained fragility curves are compared with the ones related to ESDOFs without structural variability in Figs. 12-15.

Structural variability has a notable impact on fragilities of MU1A more than the other models. MU1A model that represents well-designed 1 story masonry buildings with a very short mean period, a high mean yielding capacity and a limited mean ductility factor. For such a rigid structure with small variation in one of the parameters can cause a drastic change in the displacement response of the model. This ESDOF model becomes more vulnerable to seismic action after considering structural variability. However fragilities are generally reduced for larger PGAs after executing structural variability, regarding MU2B and MU3C. This decrease is more evident for MU2B than MU3C. The effect

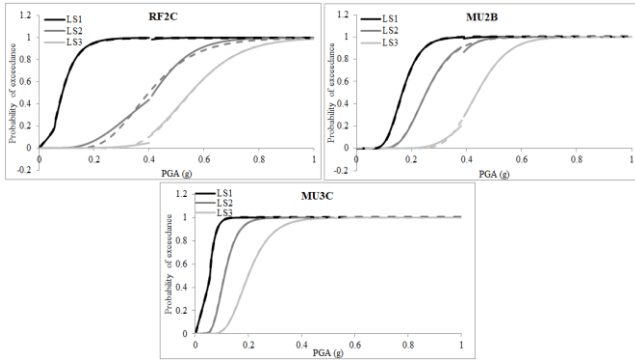


Fig. 16 Continuous fitted fragility curves (dashed line) and discontinuous original fragility curves (solid line) for Site 1 using generic site amplification (without structural variability)

of structural variability on RC frames is less evident than masonry buildings. Regarding RF2C, structural variability generally increases fragilities.

As it is obvious, fragility functions related to bilinear demand predictive models are discontinuous. The main reason of this discontinuity is two different dispersions for two line segments which is not reasonable from engineering point of view. Therefore it is recommended to fit a continuous fragility function to two separate curves. Ramamoorthy *et al.* (2006, 2008) proposed a lognormal function according to Eq. (5) to estimate the continuous fragility function.

$$\hat{F}(PGA) = \Phi\left(\frac{\ln(PGA) - \gamma_1}{\gamma_2}\right) \quad (5)$$

where $F(PGA)$ is continuous fragility function. γ_1 and γ_2 are unknown parameters which are estimated using nonlinear regression analysis by fitting $F(PGA)$ on the calculated fragilities. MATLAB program is used to fit a nonlinear curve with functional formulation of Eq. (5) on derived fragilities from the previous sections. Fig. 16 shows an example of original discontinuous fragility functions as well as fitted continuous fragility curves for Site 1 using generic site amplification and ESDOFs without structural variability. Although discontinuous fragility functions are more accurate, continuous fragility functions are recommended to be used in practical situations since they are physically more meaningful.

5. Numerical application by using Mean Damage Ratio (MDR)

The sensitivity of fragility curves to different parameters is quantified for a single ground motion scenario, in order to express it in a more tangible manner. For this purpose, damage state probabilities are calculated from fragility functions for None, Light, Moderate and Severe damage states (DSs). Continuous fragility functions are applied herein regarding bilinear predictive demand models. Fig. 17 shows damage state definitions with respect to fragility curves in this study. Dashed line shows estimated PGA

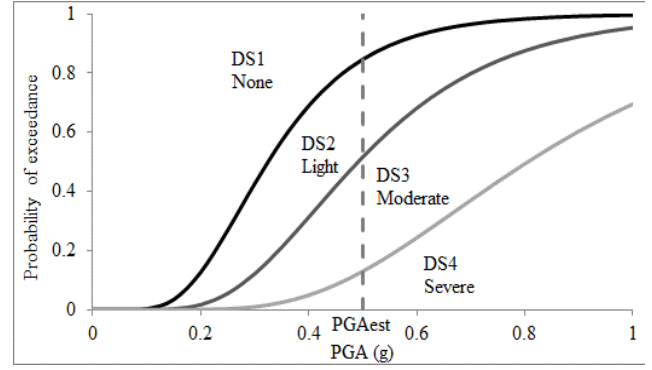


Fig. 17 Damage state definitions based on fragility functions in this study

Table 4 CDR values in this study (Adapted from Gurpinar *et al.* 1978)

Damage State	CDR (%)
None	0
Light	5
Moderate	30
Severe	70
Collapse	100

related to the ground motion scenario under study. Mean damage ratio (MDR) is defined as the weighted average of damage state probabilities and calculated using Eq. (6).

$$MDR = \sum_{i=1}^4 P(DS_i) \cdot CDR(DS_i) \quad (6)$$

where $P(DS_i)$ is the probability of i^{th} damage state, which is derived from Fig. 17. CDR is central damage ratio corresponding to each damage state. This parameter is used in order to represent the wide range of damage states with a single damage ratio. In this study, the CDR values of Gurpinar *et al.* (1978) are used, which were obtained from previous site surveys of damaged buildings in Turkey (Table 4).

Next, ground motions for the scenario of the 13 March 1992 Erzincan earthquake at Site 1 and 2 are simulated. The PGA values, which are obtained from the simulated motions, are applied to estimate damage state probabilities from fragility functions regarding each ESDOF model (with and without structural variability). MDR values for each case are then calculated according to Eq. (6) and Table 4.

Figs. 18 and 19 exhibit MDR variations of different cases from a reference case related to Site 1 and Site 2, respectively for the scenario earthquake. In Figures 18 and 19, S1, S2, T, G, $w\text{-sv}$ and $w0\text{-sv}$ stand for Site 1, Site 2, theoretical site amplification, generic site amplification, with structural variability and without structural variability.

Figs. 18 and 19 indicate that, theoretical site amplification increases MDRs of all the ESDOFs. This increase is considerable for RF2C and negligible for MU1A and MU3C. This observation is also valid after applying structural variability. It means that, theoretical site amplification is more critical than generic one for all the

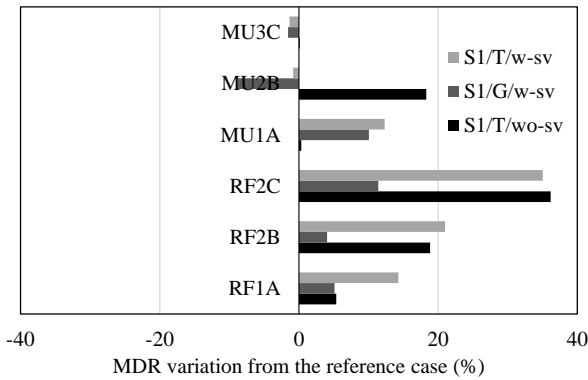


Fig. 18 MDR variation of three cases related to Site 1 from the reference case which is Site 1 using generic site amplification and without structural variability (S1/G/wo-sv)

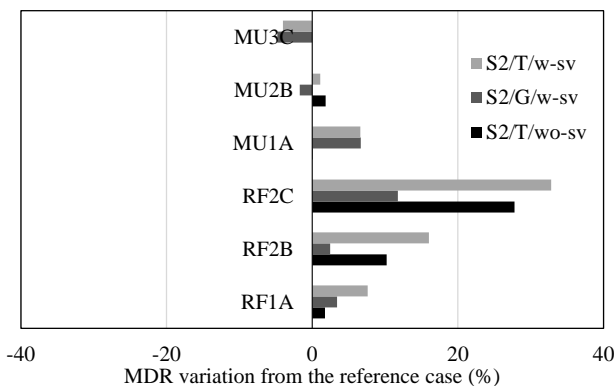


Fig. 19 MDR variation of three cases related to Site 2 from the reference case which is Site 2 using generic site amplification and without structural variability (S2/G/wo-sv)

ESDOFs with and without structural variability. Structural variability leads to larger MDRs for the ESDOFs except for MU2B and MU3C. MDR variation of MU2B with respect to theoretical site amplification and structural variability becomes smaller for Site 2.

The effect of site class on estimated damage is examined in Fig. 20. In order to eliminate the differences in hazard levels regarding different sites, a ground motion scenario with a specified PGA (=0.4 g) is utilized to estimate MDRs. Fig. 20 shows MDR errors of Site 2 from Site 1 for the ESDOF models with and without structural variability. MDR error is acquired from the variation of two MDR values divided by the smallest MDR.

It is obvious from Fig. 20 that MDR of ESDOFs at Site 1 is larger than that at Site 2 except for MU3C without structural variability. The sensitivity of RC frames to site class is more obvious than that of masonry buildings. Structural variability reduces the sensitivity of RF2C and MU2B and it grows the sensitivity of RF1A, MU1A and RF2B to site class. The effect of site class on MU3C is negligible due to failure of this model at this PGA level.

6. Conclusions

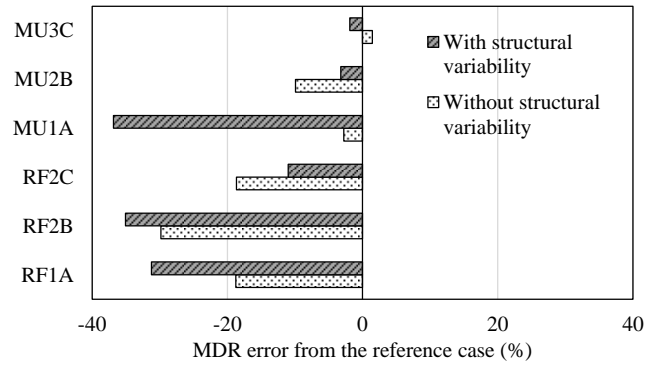


Fig. 20 MDR error of Site 2 from Site 1 for PGA=0.4 g

The use of simulated ground motions in UHS facilitates implementation of detailed site response inside probabilistic seismic hazard studies. It is difficult, however, to account for such site response models via classical PSHA as the site parameters are usually coarsely included in ground motion prediction models. Results of the regional UHS based on ground motion simulations can be useful for realistic seismic damage and loss estimations. This point is inspected through sensitivity analysis of seismic fragility functions to site conditions and local site response in this study. Typical residential buildings in Erzincan have been idealized as ESDOF systems. Predictive demand equations are developed for each ESDOF and each Site with different site amplification models. Then fragility functions of ESDOF models with and without structural variability are calculated for two sites with different site amplification models. In order to quantify the sensitivity of fragility curves to seismic and structural parameters, mean damage ratios (MDRs) of the ESDOFs with and without structural variability are calculated for two ground motion scenarios.

One of the important limitations of this study is that, stochastic ground motion simulation is preferred due to lack of detailed source descriptions and well-resolved velocity models in the case study area. This approach accounts for the inherent randomness in ground motion and is effective for high frequency region (>1 Hertz). Additionally, the buildings are idealized using ESDOF systems in this study rather than multi degree of freedom (MDOF) systems in order to reduce high computational efforts.

The following observations and conclusions are derived in this study based on the aforementioned limitations and assumptions:

- RF2C, MU2B and MU3C, which are the structural types with high degradation, require bilinear predictive demand model in most of the cases. Modifying linear models into bilinear ones for those cases improves the behavior of predictive equations in terms of R^2 .
- After implementing structural variability, MU1A becomes more vulnerable and logarithmic uncertainties become larger. Structural variability decreases the fragility functions of MU2B and MU3C at large PGAs and it increases fragilities of RF2C in most of the cases. This shows that in fragility curve generation, structural variability becomes important for both stiff structures with limited deformation capacity and for deficient

structures with severe degradation characteristics in addition to record-to-record variability.

- Site 1 leads to larger fragilities than Site 2 mostly for RC frames. Hence soft soil leads to more critical fragility functions than stiff soil especially for RC frames.
- Theoretical site amplification is more critical than generic site amplification for RC frames in terms of fragility curves. The effect of theoretical site amplification is more evident for RF2C and Site 2. The reason is high degradation characteristics of RF2C and vicinity of fundamental period of stiff site from theoretical site amplification to mid-rise RC frames.
- Fragility functions of structural models with bilinear predictive demand model are not continuous due to difference in dispersions of two linear segments. In order to overcome this issue, a lognormal nonlinear curve is fitted on discontinuous fragility curves for practical use. The lognormal function provides a suitable fit to the original discontinuous fragilities.
- The MDR variations generally confirm the above-mentioned observations corresponding to the fragility curves. Theoretical site amplification is more critical for RC frames (longer periods) than masonry buildings. Structural variability increases estimated damage of ESDOF models except for MU3C and MU2B.
- The buildings located at Site 1 (soft soil) display larger MDRs in comparison with the ones at Site 2 (stiff soil) except for MU3C. The impact of soft soil on estimated damage is more obvious for RC frames because of soil-structure interaction.

As the future studies, broad-band ground motion simulation techniques such as hybrid models might be implemented for the proposed seismic hazard and risk approach in this paper. Those techniques can be used effectively for a wide range of frequencies and fundamental periods of buildings. Besides, other structural models such as high-rise buildings or shear walls might be considered in the future.

Data and resources

EXSIM and SMSIM computer programs are downloaded from www.carleton.ca/~dariush and http://www.daveboore.com/software_online.html (last accessed on December 2014). OPENSEES program is freely available from <http://opensees.berkeley.edu/index.php> (last accessed on February 2015).

Acknowledgments

Aida Azari Sisi was a graduate student fellowship recipient of TUBITAK-2215 Program. We are grateful for this support. We also thank Shaghayegh Karimzadeh Naghshineh and Fatma Nurten Sisman Dersan for their technical support. We are grateful to David Boore and Dariush Motazedian for providing SMSIM and EXSIM as well as sharing their valuable comments during our initial applications in the past.

References

- Akansel, V.H., Ameri, G., Askan, A., Caner, A., Erdil, B., Kale, Ö. and Okuyucu, D. (2014), "The 23 October 2011 Mw 7.0 Van (eastern Turkey) earthquake: characteristics of recorded strong ground motions and post-earthquake condition assessment of infrastructure and cultural heritage", *Earthq. Spectra*, **30**(2), 657-682.
- Akcar, S. and Bommer, J. (2010), "Empirical equations for the prediction of PGA, PGV and spectral accelerations in Europe, the mediterranean region and the middle east", *Seismol. Res. Lett.*, **81**(2), 195-206.
- Ambraseys, N.N., Douglas, J., Sarma, S.K. and Smit, P.M. (2005), "Equations for the estimation of strong ground motions from shallow crustal earthquakes using data from Europe and the middle east: horizontal peak ground acceleration and spectral acceleration", *Bull. Earthq. Eng.*, **3**, 1-53.
- Ang, A.H.S. and Tang, W.H. (1975), *Probability Concepts in Engineering Planning and Design*, John Wiley and sons, Inc., New York.
- Ansal, A., Akinci, A., Gultrera, G., Erdik, M., Pessina, V., Tonuk, G. and Ameri, G. (2009), "Loss estimation in Istanbul based on deterministic earthquake scenarios of the Marmara sea region (Turkey)", *Soil Dyn. Earthq. Eng.*, **29**, 699-709.
- Askan, A., Asten, M., Erberik, M.A., Erkmek, C., Karimzadeh, S., Kılıç, N., Şişman, F.N. and Yakut, A. (2015), "Estimation of potential seismic damage in Erzincan", Final Report of TUJJB-UDP-01-12 Project, Ankara.
- Askan, A., Sisman, F.N. and Ugurhan, B. (2013), "Stochastic strong ground motion simulations in sparsely-monitored regions: a validation and sensitivity study on the 13 March 1992 Erzincan (Turkey) earthquake", *Soil Dyn. Earthq. Eng.*, **55**, 170-181.
- Ay, B.O. and Erberik, M.A. (2008), "Vulnerability of Turkish low-rise and mid-rise reinforced concrete frame structures", *J. Earthq. Eng.*, **12**(S2), 2-11.
- Ayyub, B.M. and Lai, K. (1989), "Structural reliability assessment using latin hypercube sampling", *Proceedings of the 5th International Conference on Structural Safety and Reliability*, San Francisco, United States.
- Azari Sisi, A., Askan, A. and Erberik, M.A. (2017), "Site-specific uniform hazard spectrum in eastern Turkey based on simulated ground motions including near-field directivity and detailed site effects", *Acta Geophysica*, **65**(2), 309-330.
- Bai, J.W., Gardoni, P. and Hueste, M.B. (2011), "Story-specific demand models and seismic fragility estimates for multi-story buildings", *Struct. Saf.*, **33**, 96-107.
- Boore, M.D. (2003), "Simulation of ground motion using the stochastic method", *Pure Appl. Geophys.*, **160**(3-4), 635-676.
- Boore, M.D. and Joyner, W.B. (1997), "Site amplifications for generic rock sites", *Bull. Seismol. Soc. Am.*, **87**(2), 327-341.
- Celik, O.C. and Ellingwood, B.R. (2010), "Seismic fragilities for non-ductile reinforced concrete frames-role of aleatoric and epistemic uncertainties", *Struct. Saf.*, **32**, 1-12.
- Cramer, C.H. (2006), "Quantifying the uncertainty in site amplification modeling and its effects on site-specific seismic-hazard estimation in the upper Mississippi embayment and adjacent areas", *Bull. Seismol. Soc. Am.*, **96**(6), 2008-2020.
- Crowley, H., Bommer, J., Pinho, R. and Bird, J. (2005), "The impact of epistemic uncertainty on an earthquake loss model", *Earthq. Eng. Struct. Dyn.*, **34**, 1653-1685.
- Deniz, A. (2006), "Estimation of earthquake insurance premium rates based on stochastic methods", Master of Science, Middle East Technical University, Ankara.
- Ellingwood, B.R., Celik, O.C. and Kinali, K. (2007), "Fragility assessment of building structural systems in mid-America", *Earthq. Eng. Struct. Dyn.*, **36**, 1935-1952.

- Erberik, M.A. (2008a), "Fragility-based assessment of typical mid-rise and low-rise RC buildings in Turkey", *Eng. Struct.*, **30**(5), 1360-1374.
- Erberik, M.A. (2008b), "Generation of fragility curves for Turkish masonry buildings considering in-plane failure modes", *Earthq. Eng. Struct. Dyn.*, **37**(3), 387-405.
- Gurpinar, A., Abali, M., Yucemen, M.S. and Yesilcay, Y. (1978), "Feasibility of mandatory earthquake insurance in Turkey", Earthquake Engineering Research Center.
- Hashash, Y. and Moon, S. (2011), "Site amplification factors for deep deposits and their application in seismic hazard analysis for Central U.S", University of Illinois at Urbana-Champaign, Urbana.
- Ibarra, L., Medina, R. and Krawinkler, H. (2005), "Hysteretic models that incorporate strength and stiffness deterioration", *Earthq. Eng. Struct. Dyn.*, **34**, 1489-1511.
- Jeong, J., Park, J. and DesRoches, R. (2015), "Seismic fragility of lightly reinforced concrete frames with masonry infills", *Earthq. Eng. Struct. Dyn.*, **44**(11), 1783-1803.
- Krawinkler, H., Medina, R. and Alavi, B. (2003), "Seismic drift and ductility demands and their dependence on ground motions," *Eng. Struct.*, **25**(5), 637-653.
- Marthong, C., Deb, S.K. and Dutta, A. (2016), "Experimental fragility functions for exterior deficient RC beamcolumn connections before and after rehabilitation", *Earthq. Struct.*, **10**(6), 1291-1314.
- McKay, M.D., Beckman, R.J. and Conover, W.J. (1979), "A comparison of three methods for selecting values of input variables in the analysis of output from a computer code", *Technom.*, **21**(2), 239-245.
- Mohammadioun, B. and Serva, L. (2001), "Stress drop, slip type, earthquake magnitude, and seismic hazard", *Bull. Seismol. Soc. Am.*, **91**(4), 604-707.
- Mosleh, A., Razzaghi, M.S., Jara, J. and Varum, H. (2016), "Development of fragility curves for RC bridges subjected to reverse and strike-slip seismic sources", *Earthq. Struct.*, **11**(3), 517-538.
- Motazedian, D. and Atkinson, G.M. (2005), "Stochastic finite-fault modeling based on a dynamic corner frequency", *Bull. Seismol. Soc. Am.*, **95**(3), 995-1010.
- Nagashree B.K., Ravi Kumar, C.M. and Venkat Reddy, D. (2016), "A parametric study on seismic fragility analysis of RC buildings", *Earthq. Struct.*, **10**(3), 629-643.
- Padgett, J.E. and DesRoches, R. (2007), "Sensitivity of seismic response and fragility to parameter uncertainty", *J. Struct. Eng.*, **133**(12), 1710-1718.
- Porter, K.A. (2003), *Seismic Vulnerability*, Earthquake Engineering Handbook, Eds. W.F. Chan and C. Scawthorn, CRC Press, Boca Raton, FL.
- Ramamoorthy, S.K., Gardoni, P. and Bracci, J.M. (2006), "Probabilistic demand models and fragility curves for reinforced concrete frames", *J. Struct. Eng.*, **132**(10), 1563-1572.
- Ramamoorthy, S.K., Gardoni, P. and Bracci, J.M. (2008), "Seismic fragility and confidence bounds for gravity load designed reinforced concrete frames of varying height", *J. Struct. Eng.*, **134**(4), 639-650.
- Raschke, M. (2014), "Insufficient statistical model development of ground-motion relations for regions with low seismicity", *Bull. Seismol. Soc. Am.*, **104**(2), 1002-1005.
- Rohmer, J., Douglas, J., Bertil, D., Monfort, D. and Sedan, O. (2014), "Weighing the importance of model uncertainty against parameter uncertainty in earthquake loss assessments", *Soil Dyn. Earthq. Eng.*, **58**, 1-9.
- Schnabel, P.B., Lysmer, J. and Seed, H.B. (1972), "SHAKE: A computer program for earthquake response analysis of horizontally layered sites", Earthquake Engineering Research Center, University of California, Berkeley, USA.
- Ugurhan, B., Askan Gundogan, A. and Erberik, M.A. (2011), "A methodology for seismic loss estimation in urban regions based on ground-motion simulations", *Bull. Seismol. Soc. Am.*, **101**(2), 701-725.
- Wells, D.L. and Coppersmith, K.J. (1994), "New empirical relationships among magnitude, rupture length, rupture width, rupture area and surface displacement", *Bull. Seismol. Soc. Am.*, **84**(4), 974-1002.
- Wen, Y.K., Ellingwood, B.R. and Bracci, J.M. (2004), "Vulnerability function framework for consequence-based engineering", MAE Center Project DS-4 Report.

AT